





# The valve uptake index: improving assessment of prosthetic valve endocarditis and updating [<sup>18</sup>F]FDG PET/CT(A) imaging criteria

Albert Roque <sup>1,2,3,4,\*</sup>, María N. Pizzi <sup>3,4,5,6</sup>, Nuria Fernández-Hidalgo <sup>3,4,7</sup>, Guillermo Romero-Farina <sup>4,5</sup>, Gemma Burcet<sup>1,2,3,4</sup>, José Luis Reyes-Juarez<sup>1,2,3,4</sup>, Carina Espinet<sup>2,3,8</sup>, Joan Castell-Conesa<sup>2,3,8</sup>, Manuel Escobar<sup>1,2</sup>, Ignacio Ferreira-González<sup>3,5,9</sup>, Santiago Aguadé-Bruix<sup>3,4,6,8</sup>, and Hug Cuellar-Calabria<sup>1,2,3,4</sup>

<sup>1</sup>Department of Radiology, Hospital Universitari Vall d'Hebron, Passeig Vall d'Hebron 119-129, 08035 Barcelona, Spain; <sup>2</sup>IDI (Institut de Diagnòstic per la Imatge), Barcelona, Spain; <sup>3</sup>Departament de Medicina, Universitat Autònoma de Barcelona, Passeig Vall d'Hebron 119-129, 08035 Barcelona, Spain; <sup>4</sup>Vall d'Hebron Institut de Recerca (VHIR), Passeig Vall d'Hebron 119-129, 08035 Barcelona, Spain; <sup>5</sup>Department of Cardiology, Hospital Universitari Vall d'Hebron, Passeig Vall d'Hebron 119-129, 08035 Barcelona, Spain; <sup>6</sup>Centro de Investigación Biomédica en Red en Enfermedades Cardiovasculares (CIBERCV), Madrid, Spain; <sup>7</sup>Department of Infectious Diseases, Hospital Universitari Vall d'Hebron, Passeig Vall d'Hebron 119-129, 08035 Barcelona, Spain; <sup>8</sup>Department of Nuclear Medicine, Hospital Universitari Vall d'Hebron, Passeig Vall d'Hebron 119-129, 08035 Barcelona, Spain; and <sup>9</sup>CIBER de Epidemiología y Salud Pública (CIBERESP), Madrid, Spain

Received 23 September 2021; editorial decision 10 December 2021; accepted 13 December 2021; online publish-ahead-of-print 6 January 2022

## Aims

Diagnosis of prosthetic valve endocarditis (PVE) by positron emission computed tomography angiography (PET/CTA) is based on visual and quantitative morpho-metabolic features. However, the fluorodeoxyglucose (FDG) uptake pattern can be sometimes visually unclear and susceptible to subjectivity. This study aimed to validate a new parameter, the valve uptake index [VUI, maximum standardized uptake value (SUVmax)-mean standardized uptake value (SUVmean)/SUVmax], designed to provide a more objective indication of the distribution of metabolic activity. Secondly, to re-evaluate the utility of traditionally used PVE imaging criteria and determine the potential value of adding the VUI in the diagnostic algorithm of PVE.

## Methods and results

Retrospective analysis of 122 patients (135 prosthetic valves) admitted for suspicion of endocarditis, with a conclusive diagnosis of definite ( $N=57$ ) or rejected ( $N=65$ ) PVE, and who had undergone a cardiac PET/CTA scan as part of the diagnostic evaluation. We measured the VUI and recorded the SUVmax, SUVratio, uptake pattern, and the presence of endocarditis-related anatomic lesions. The VUI, SUVmax, and SUVratio values were  $0.54 \pm 0.1$  vs.  $0.36 \pm 0.08$ ,  $7.68 \pm 3.07$  vs.  $3.72 \pm 1.11$ , and  $4.28 \pm 1.93$  vs.  $2.16 \pm 0.95$  in the 'definite' PVE group vs. the 'rejected' group, respectively (mean  $\pm$  SD;  $P < 0.001$ ). A cut-off value of VUI  $> 0.45$  showed a sensitivity, specificity, and diagnostic accuracy for PVE of 85%, 88%, and 86.7% and increased diagnostic ability for confirming endocarditis when combined with the standard diagnostic criteria.

## Conclusions

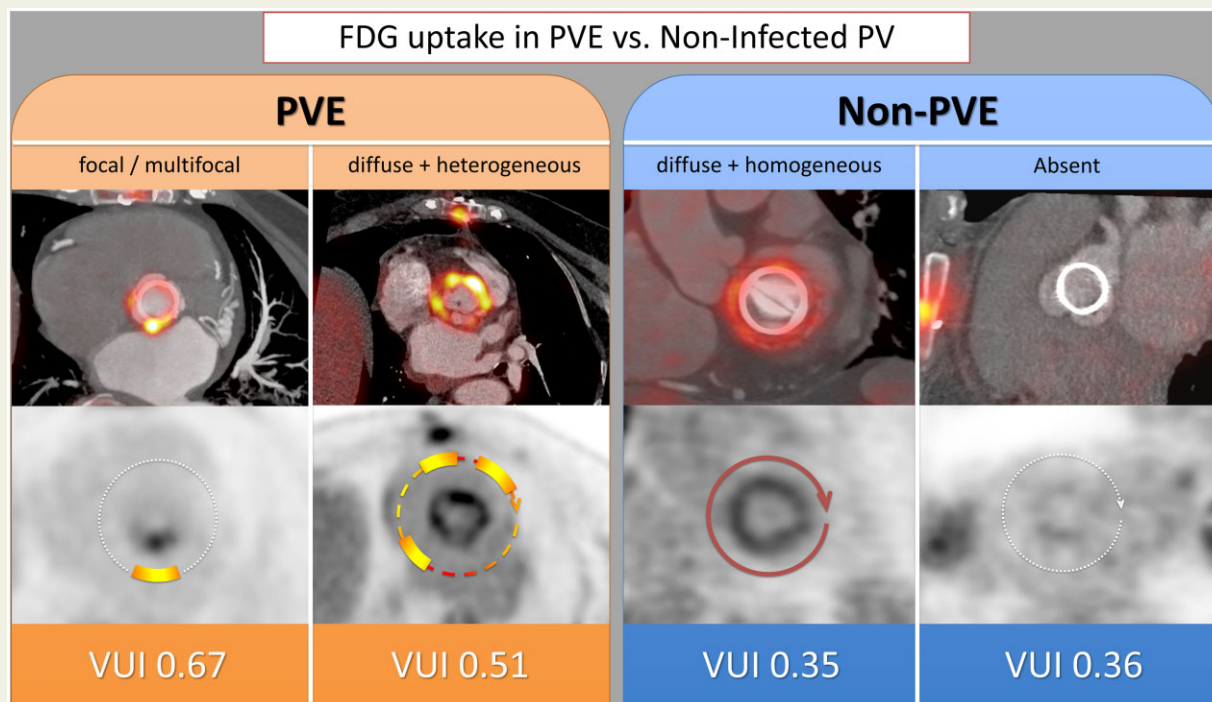
The VUI demonstrated good diagnostic accuracy for PVE, even increasing the diagnostic power of the traditionally used morphometabolic parameters, which also confirmed their own diagnostic performance. More research is needed to assess whether the integration of the VUI into the PVE diagnostic algorithm may clarify doubtful cases and thus improve the diagnostic yield of PET/CTA.

\*Corresponding author. Tel: +34 932746029; Fax: +34 932746764. E-mail: albert\_roque@hotmail.com

© The Author(s) 2022. Published by Oxford University Press on behalf of the European Society of Cardiology.

This is an Open Access article distributed under the terms of the Creative Commons Attribution-NonCommercial License (<https://creativecommons.org/licenses/by-nc/4.0/>), which permits non-commercial re-use, distribution, and reproduction in any medium, provided the original work is properly cited. For commercial re-use, please contact [journals.permissions@oup.com](mailto:journals.permissions@oup.com)

## Graphical Abstract



## Keywords

prosthetic heart valves • positron emission tomography • infective endocarditis • nuclear imaging

## Introduction

Positron emission computed tomography with  $^{18}\text{F}$ -fluorodeoxyglucose ( $^{18}\text{F}$ FDG PET/CT) associated with ECG-gated cardiac CT angiography (PET/CTA) has significantly improved the diagnostic yield of prosthetic valve endocarditis (PVE) when combined with the Duke criteria.<sup>1,2</sup> Hence, PET/CT findings have been incorporated in the 2015 ESC and in the 2020 ACC/AHA guidelines for the diagnosis of infective endocarditis (IE).<sup>3,4</sup> It is known that FDG uptake can be often present in non-infected prosthetic valves (PVs), especially in the recent postoperative period, with the potential risk of misinterpreting reactive inflammation as infection.<sup>5</sup> Nevertheless, FDG uptake in non-infected PVs is usually diffuse, homogeneous and of mild intensity, and differs from the focal/heterogeneous uptake normally seen in PVE. The combination of a considered-normal uptake pattern with the absence of anatomic lesions on CTA (the two proposed 'major criteria of normality') are the cornerstones of PV evaluation by PET/CTA, and usually allows postoperative inflammation to be distinguished from active infection.<sup>5-8</sup> Thus, if PET/CT is not combined with cardiac CTA, the uptake pattern would remain as the main criterion to classify a PET/CT scan as positive or negative for IE. Since assessment of the FDG distribution is basically visual, it may be open to subjectivity and occasionally unclear, hampering its classification as homogeneous or heterogeneous pattern. Therefore, in addition to qualitative assessment, it would be desirable to have a

reference parameter providing a more objective indication of the distribution of metabolic activity, which is not well reflected by standardized uptake values (SUVs).<sup>9</sup> We recently developed a new measure, the 'valve uptake index' (VUI), first evaluated in a cohort of patients without suspected infection who underwent serial cardiac PET/CTA examinations after PV implantation surgery.<sup>5</sup> The VUI provided information about the degree of homogeneity of the metabolic activity, as it attenuates the effect of high SUV values when uptake is diffuse. The main aim of this study was to validate the utility of this index in patients with suspicion of PVE and establish cut-off values to determine when a PV shows normal uptake (low probability of infection) or abnormal uptake (high probability of PVE). In addition, we re-evaluated the traditionally used PVE imaging findings to establish the PET/CTA imaging criteria for infection.

## Methods

We performed a retrospective analysis of 135 patients with suspicion of PVE admitted to our IE-referral hospital between February 2013 and February 2020, and who underwent cardiac PET/CTA as part of the diagnostic work-up. In order to determine how the VUI correlated with the visual pattern, only patients with a clearly classifiable uptake pattern were included. Besides, only patients with a final conclusive diagnosis of 'definite' ( $N=57$ ) or 'rejected' ( $N=65$ ) PVE by the Expert Team after a 6-month follow-up were analysed, while inconclusive cases ('possible' PVE,

13) were excluded. In patients with double mitroaortic PV replacement ( $n = 17$ ), the analysis was performed in both prostheses in the 'rejected' group (10/17), in both prostheses in the 'definite' group with mitroaortic endocarditis (3/17), but only in the involved PV in the remaining cases (4/17). Finally, a total of 75 rejected and 60 definite PVs were analysed (enrolment flowchart is shown in Figure 1).

The study protocol was approved by the hospital ethics committee, and written informed consent was obtained from all participants.

## PET/CTA technical considerations and image interpretation

Patients underwent specific cardiac [ $^{18}\text{F}$ ]FDG PET/CTA including myocardial FDG suppression measures and the combination of both metabolic (PET) and anatomic (CTA) ECG-gated cardiac acquisitions, as previously described.<sup>10-12</sup> Fused PET/CTA images were evaluated by two experienced cardiac imaging specialists, a cardiac radiologist and a nuclear cardiologist. Double-oblique planes were used to obtain transverse views of the PVs.

## Visual (non-quantitative) analysis: metabolic pattern and anatomic lesions

The prosthetic/periprosthetic [ $^{18}\text{F}$ ]FDG uptake pattern was visually analysed in attenuation correction (AC), localized ECG-gated cardiac (C-Bed), and non-attenuation correction (NAC) images, and was

classified as: 'absent', 'focal/multifocal', or 'diffuse', with the latter being further sub-classified into 'homogeneous' or 'heterogeneous', as previously defined.<sup>9,10</sup> Focal/multifocal and diffuse-heterogeneous distributions are considered 'abnormal patterns' suggestive of infection, against absent and diffuse-homogenous uptakes that are considered 'normal patterns'. CTA images were systematically evaluated to detect IE-related anatomic lesions (vegetations, abscesses, pseudoaneurysms, and fistulae).

## Quantitative analysis: uptake intensity and VUI

Quantification was made on a circular region of interest (ROI) manually adjusted to encompass the PV, and drawn on a 10 mm thick maximum intensity projection (MIP) transverse view of the valve plane in the morpho-metabolic fusion images. Two sets of metabolic acquisitions were used for the fusion: the standard AC images commonly used in PET/CT for other purposes, and a localized ECG-gated cardiac bed (C-Bed) to improve evaluation of cardiac structures. The standard maximum and mean standardized uptake values (SUVmax and SUVmean) were collected. The target-to-background ratio (SUVratio) was calculated as the ratio between the SUVmax of the valve and the SUVmean of the blood pool in the left atrium. Finally, we obtained the valve uptake index (VUI), first described in our previous control group<sup>5</sup> and calculated as follows:  $(\text{SUVmax} - \text{SUVmean}) / \text{SUVmax}$  (Figure 2). As the images most commonly used worldwide are those of AC, the statistical analysis was performed with the values obtained in these reconstructions, with the aim of making

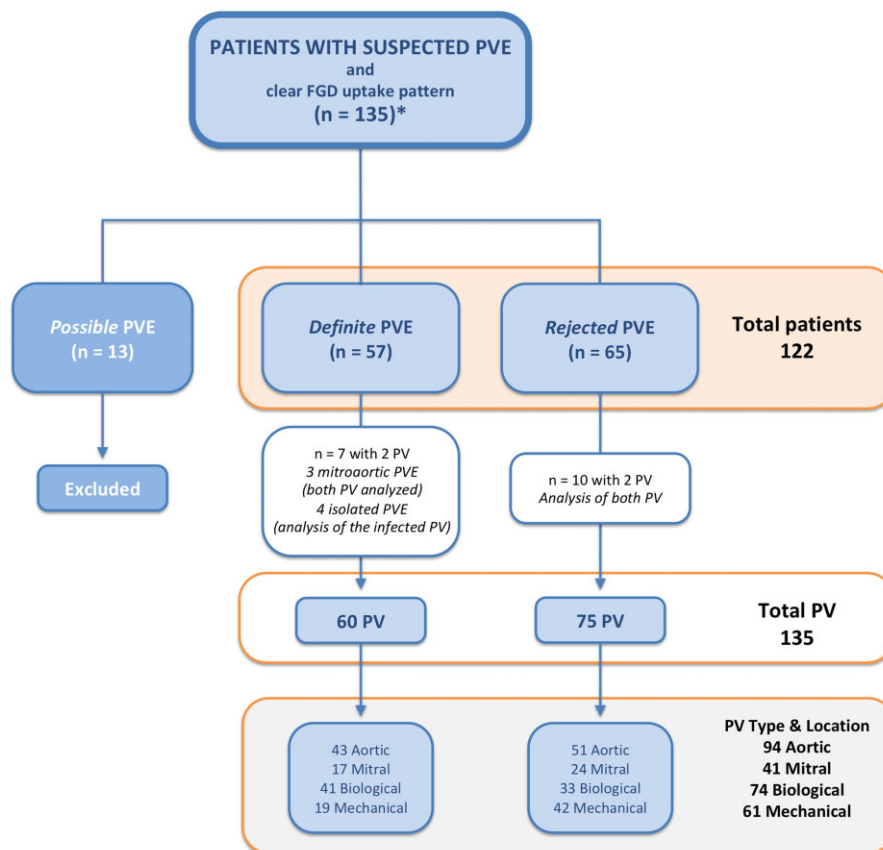


**Figure 1** Study flowchart. \*From our tertiary referral hospital for infective endocarditis with an estimated volume of 60 definite endocarditis per year, of which approximately 25 definite PVE per year. PV, prosthetic heart valve; PVE, prosthetic valve endocarditis.

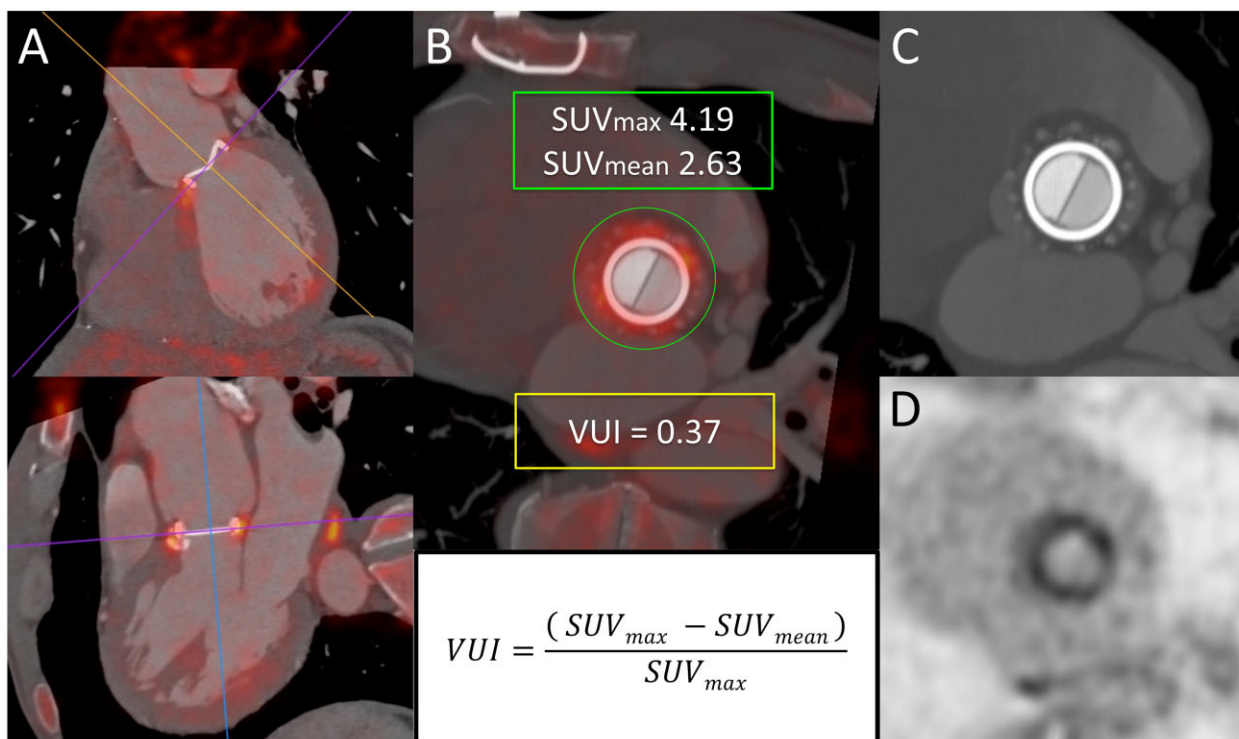


**Figure 2** PET/CTA systematic evaluation. Visual (non-quantitative) and quantitative analysis of an aortic mechanical prosthetic valve. (A, top and bottom) Multiplanar reformation of PET/CTA fusion images to obtain a transverse view of the prosthesis. A diffuse and homogeneous FDG uptake pattern is seen in both fusion (B) and attenuation-corrected PET images (D). (C) Cardiac CTA shows no associated anatomic lesions. (B) A circular region of interest drawn on the valve plane allows the SUV<sub>max</sub> and SUV<sub>mean</sub> to be obtained, from which the VUI is subsequently calculated (formula). FDG, fluorodeoxyglucose; PET/CTA, positron emission computed tomography angiography; SUV<sub>max</sub> and SUV<sub>mean</sub>, maximum and mean standardized uptake value; VUI, valve uptake index.

them more exportable. The intra-class correlation coefficient agreement between the two observers for VUI measurements was computed. Details on quantification procedure are supplied in [Supplementary data online, Material I and Videos](#).

### Statistical analysis

All continuous data are expressed as mean (standard deviation), and all non-continuous variables are expressed as percentages. Continuous variables were compared using the *t*-test for unpaired samples. Differences between proportions were compared using the  $\chi^2$  test.

First, we evaluated the diagnostic accuracy of a VUI > 0.45 for PVE, a value that we previously described to be the mean + 1SD VUI (0.35 ± 0.1) in non-infected prosthetic heart valves.<sup>5</sup>

Then we analysed both the qualitative and quantitative variables of the PET/CTA images routinely used for the diagnosis of IE. Multiple logistic regression models were analysed to predict PVE. Forward stepwise selection techniques (FSTEP) were used to identify which variables were independently associated with IE. The threshold for variable entry into all multivariable models was a *P*-value < 0.05 and that for variable removal was a *P*-value > 0.10. All models were adjusted for age and PV type, and the area under the curve (AUC) was calculated. Models were considered reasonable when the AUC was > 0.7 and strong when it exceeded 0.8.

A value of *P* < 0.05 was considered as indicative of statistical significance. All statistical tests were two-sided. The data were analysed using Stata 15 (College Station, TX, USA).

## Results

### Study population and patient characteristics

A total of 122 patients under suspicion of PVE who underwent a cardiac PET/CTA, with a classifiable FDG uptake pattern and a final conclusive diagnosis of 'confirmed or rejected' IE were included in the analysis. Of the 122 patients under suspicion of PVE, 60 prostheses were analysed in the 'definite' group (aortic-mitral/biological-mechanical: 43-17/41-19) and 75 in the 'rejected' group (51-24/33-42). The most frequent pathogens identified were coagulase-negative staphylococci (17/57, 29.8%, mainly *Staphylococcus epidermidis*), and *Enterococcus faecalis* (14/57, 24.6%), followed by *Streptococcus* spp. (10/57, 17.5%). The included patients, PV type and location are shown in [Figure 1](#) and are described in [Table 1](#).

### Visual (non-quantitative) analysis: metabolic pattern and anatomic lesions

Prosthetic/periprosthetic FDG uptake was visually detected in all 60 (100%) 'definite' PVE, but in only 26/75 (35%) of the 'rejected' group. The FDG uptake pattern was 'focal/multifocal' in 34/60 (57%), 'diffuse-heterogeneous' in 24/60 (40%) and 'diffuse-homogeneous' in

**Table 1** Patient characteristics, study parameters, and morpho-metabolic findings

According to final diagnosis (n = 122 patients)	Definite PVE (n = 57)	Rejected PVE (n = 65)		
Clinical and study characteristics				
Age (years), mean ± SD	73 ± 5	69 ± 14		
Men, n (%)	34 (60)	41 (63)		
Symptoms highly suggestive of PVE (2015-ESC diagnostic criteria <sup>a</sup> ), n (%)	57 (100)	55 (85)		
Positive microbiological findings at completion of follow-up, <sup>b</sup> n (%)	57 (100)	39 (60)		
Time from symptom onset-PET/CTA (days), median (IQR) <sup>c</sup>	19 (10–41)	19 (11–37)		
Days of antibiotics-PET/CTA, mean ± SD	11 ± 12	9 ± 8		
[ <sup>18</sup> F]FDG myocardial suppression, adequate, <sup>d</sup> n (%)	56 (98)	50 (77)		
<b>According to final diagnosis (n = 135 prosthesis)</b>	<b>(n = 60)</b>	<b>(n = 75)</b>		
Position and type of prosthesis				
Aortic (n = 94)	43	51		
Mitral (n = 41)	17	24		
Biological (n = 74)	41	33		
Mechanical (n = 61)	19	42		
Time from surgery to PET/CTA (months), median (IQR)	35 (8–81)	49 (5–134)		
<1 year, n (%)	23 (38)	27 (36)		
≥1 year, n (%)	37 (62)	48 (64)		
<b>Visual (Non-quantitative) analysis</b>				
Metabolic pattern ([ <sup>18</sup> F]FDG distribution), n (%)				
Any visually detected activity	60 (100)	26 (35)		
Absence of uptake	0 (0)	49 (65)		
Focal or multifocal uptake	34 (57)	2 (3)		
Diffuse heterogeneous uptake	24 (40)	1 (1)		
Diffuse homogeneous uptake	2 (3)	23 (31)		
Anatomic lesions, n (%)				
Any IE-related lesion	39 (65)	9 (12)		
Images consistent with vegetations	19/39 (49)	2/9 (22)		
Abscesses	26/39 (67)	0 (0)		
Pseudoaneurysms	13/39 (33)	3/9 (33)		
Fistulae	3/39 (8)	4/9 (44)		
Number of lesions per patients (when present)				
1 lesion	19 (49)	7 (9)		
2 lesions	15 (38)	1 (1)		
3 lesions	5 (13)	0		
Distant/peripheral lesions (embolic or metastatic lesions), n (%)	17/57 (30)	3/65 (5)		
<b>Quantitative analysis [<sup>18</sup>F] FDG uptake intensity and VUI, mean ± SD</b>				
SUVmax AC images	7.68 ± 3.07	3.72 ± 1.11		
SUVmax C-Bed <sup>e</sup> images	7.95 ± 3.4	3.64 ± 1.28		
SUVmean AC images	3.29 ± 0.94	2.38 ± 0.7		
SUVmean C-Bed images	3.5 ± 1.12	2.41 ± 0.82		
SUVratio <sup>f</sup> AC images	4.28 ± 1.93	2.16 ± 0.95		
SUVratio C-Bed images	4.73 ± 2.29	2.3 ± 1.03		
VUI <sup>g</sup> AC images	0.54 ± 0.1	0.36 ± 0.08		
VUI C-Bed images	0.53 ± 0.1	0.34 ± 0.07		
<b>According to prosthesis position and type</b>	<b>Aortic</b>	<b>Mitral</b>	<b>Aortic</b>	<b>Mitral</b>
SUVmax AC, mean ± SD				
Biological	8.19 ± 3.24	9.97 ± 2.42	3.7 ± 0.86	4.3 ± 0.25
Mechanical	6.11 ± 2.59	5.77 ± 1.37	3.57 ± 1.22	3.77 ± 1.24
SUVratio AC, mean ± SD				
Biological	4.39 ± 1.78	5.27 ± 2.22	2.11 ± 1.03	2.41 ± 0.53
Mechanical	3.56 ± 1.9	3.88 ± 2.18	2.36 ± 1.1	2.2 ± 0.86

Continued

**Table 1 Continued**

According to prosthesis position and type		Aortic	Mitral	Aortic	Mitral
VUI AC, mean ± SD	Biological	0.54 ± 0.09	0.64 ± 0.1	0.31 ± 0.06	0.4 ± 0.07
	Mechanical	0.50 ± 0.11	0.54 ± 0.08	0.35 ± 0.07	0.41 ± 0.07

<sup>a</sup>2015-ESC diagnostic criteria,<sup>3</sup> considered symptoms (temperature >38°C, heart failure, peripheral symptoms, and septic shock).

<sup>b</sup>Positive blood cultures at admission or during clinical course or positive cultures of surgical material.

<sup>c</sup>25th–75th interquartile.

<sup>d</sup>Adequate myocardial suppression was defined as complete suppression or partial suppression that did not interfere with PV evaluation.

<sup>e</sup>Cardiac C-Bed.

<sup>f</sup>Prosthesis-to-background (blood pool) SUV ratio.

<sup>g</sup>AC, attenuation correction; IE, infective endocarditis; PET/CTA, positron emission computed tomography angiography; SUVmax, maximum standardized uptake value; [18F]FDG, 18F-fluorodeoxyglucose; VUI, valve uptake index.

2/60 (3%) in the definite group, and was absent in 49/75 (65%), ‘diffuse-homogeneous’ in 23/75 (31%), ‘focal/multifocal’ in 2/75 (3%), and ‘diffuse-heterogeneous’ in 1/75 (1%) in the ‘rejected’ group. All cases of positive FDG uptake visualized in the AC and C-Bed images were also identified in NAC images.

In the multiple logistic regression analysis (included variables: focal, heterogeneous and homogeneous patterns, and anatomic lesions), focal pattern ( $X^2$ : 37.445;  $P < 0.001$ ; S 56.7%, E 97.3%, AUC 0.79) was an independent predictor for PVE followed by the heterogeneous pattern ( $X^2$ : 28.222;  $P < 0.001$ ; S 40%, E 98.7%, AUC 0.73); adjusted by age and PV type. Although in clinical practice, a prosthesis can only display one pattern per episode (Supplementary data online, Figure S1), both the focal/multifocal and the heterogeneous patterns are ‘a priori’ ‘abnormal’ and, when evaluated as a group, its high diagnostic power (AUC 0.96) confirms the relevance of the visual criteria (Table 2 and Figure 3).

Cardiac CTA images showed IE-related lesions in 39 out of 60 (65%) definite PVE cases, of which 19 (49%), 15 (38%), and 5 (13%) patients showed 1, 2, or 3 anatomic lesions, respectively, with peri-prosthetic abscess being the most frequently identified lesion. The presence of these anatomic lesions showed 65% sensitivity, 90.7%

specificity and 0.79 AUC (CI 0.72–0.85) for the diagnosis of PVE (Figure 4A). Conversely, lesions were identified in only 8 out of 75 (11%) of the rejected cases: 7 patients (9%) showed 1 lesion and 1 patient (1%) showed 2 lesions, with fistula being the most frequent.

A description of the FDG uptake patterns and type and frequency of anatomic lesions for each group and according to valve position and type are shown in Table 1.

### Quantitative analysis: uptake intensity and VUI

Mean ± SD uptake values (AC images) for the ‘definite’ PVE group and the ‘rejected’ group were: SUVmax 7.68 ± 3.07 vs. 3.72 ± 1.11, SUVmean 3.29 ± 0.94 vs. 2.38 ± 0.7, SUVratio 4.28 ± 1.93 vs. 2.16 ± 0.95, and VUI 0.54 ± 0.1 vs. 0.36 ± 0.08. These differences were all statistically significant ( $P < 0.001$ ). Values calculated in the C-Bed images are summarized in Table 1. No differences were found in uptake values related to valve type (mechanical or biological;  $P = 0.3$ ) or position (aortic or mitral;  $P = 0.21$ ) in either in the ‘definite’ or the ‘rejected’ group. There was an excellent absolute agreement

**Table 2 Results of diagnostic ability of each quantitative and qualitative parameter analysed and with the addition of the VUI**

	Sensitivity (%CI)	Specificity (%CI)	Accuracy (%CI)
<b>Qualitative parameters</b>			
Focal pattern	56.7 (44.1–68.4)	97.3 (90.8–99.3)	79.3 (71.7–85.2)
Heterogeneous pattern	40 (28.6–52.6)	98.7 (92.8–99.8)	72.6 (64.5–79.4)
Abnormal patterns (focal OR heterogeneous uptake)	96.7 (88.6–99.1)	96 (88.9–98.6)	96.3 (91.6–98.4)
Anatomic lesions	65 (52.4–75.8)	90.7 (81.9–95.4)	79.3 (71.6–85.2)
<b>Quantitative parameters</b>			
(attenuation correction images, AC)			
SUVmax	83.3 (71.9–90.7)	88 (78.7–93.6)	85.9 (79.1–90.8)
SUVmax >5.28	84.3 (74.5–90.9)	83.3 (74.2–88.9)	84.1 (77.6–88.6)
SUVratio	80 (68.2–88.2)	90.7 (81.9–95.4)	85.9 (79.1–90.8)
SUVratio >2.58	84 (72.2–90.4)	77.2 (67.6–84.1)	79.7 (72.6–84.9)
VUI	83.3 (71.9–90.7)	93.3 (85.3–97.1)	88.9 (82.5–93.2)
VUI >0.45	85 (73.9–91.9)	88 (78.7–93.6)	86.7 (79.9–91.4)
<b>Qualitative parameters + VUI &gt;0.45</b>			
Focal pattern + VUI >0.45	95 (86.3–98.3)	86.7 (77.2–92.6)	90.4 (84.2–94.3)
Heterogeneous pattern + VUI >0.45	86.7 (75.8–93.1)	87 (77.2–92.6)	86.7 (79.9–91.4)
Anatomic lesions + VUI >0.45	85 (73.9–91.9)	88 (78.7–93.6)	86.7 (80–91)

All values adjusted by age and prosthesis type. SUVmax, maximum standardized uptake value; VUI, valve uptake index.

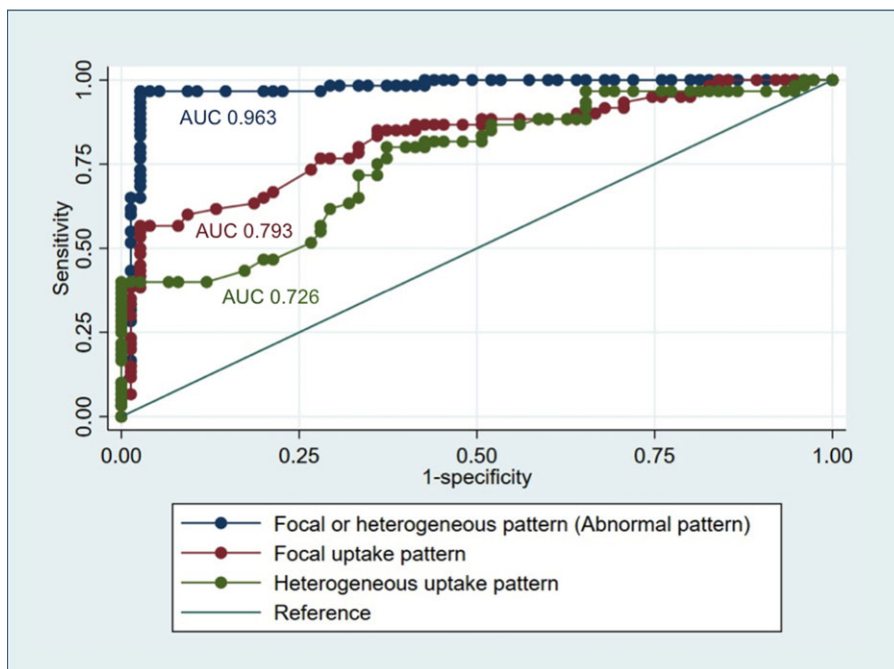


**Figure 3** Receiver–operator characteristics (ROC) curves showing the PVE diagnostic accuracy of the focal and the heterogeneous pattern individually (red and green curves, respectively) and the focal OR heterogeneous patterns considered as a group of *abnormal* FDG uptake (blue curve). FDG, fluorodeoxyglucose; PVE, prosthetic valve endocarditis.

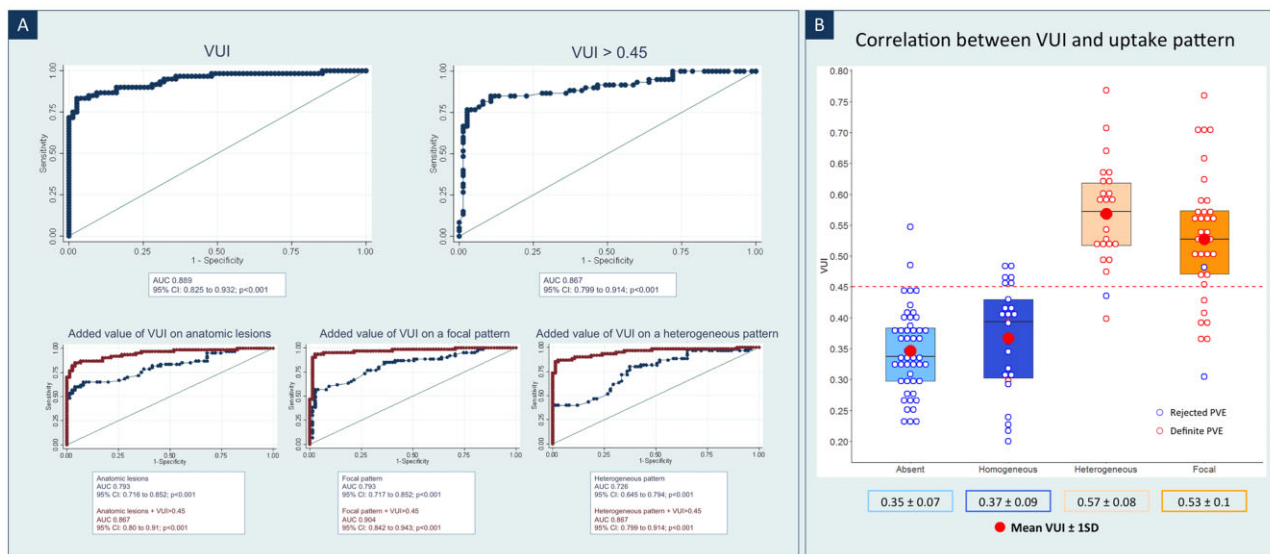


**Figure 4** (A) Receiver–operator characteristics (ROC) curves showing the PVE diagnostic accuracy of the VUI and VUI > 0.45 cut-off value (upper row). Added value of the VUI to the qualitative parameters (bottom row). (B) Mean  $\pm$  SD VUI values according to the FDG uptake pattern and distribution of rejected and definite cases. Focal and heterogeneous patterns correlate with significantly higher VUI values in comparison with absent and homogenous patterns. FDG, fluorodeoxyglucose; PVE, prosthetic valve endocarditis; VUI, valve uptake index.

between the observers, using the two-way random effect models and 'single rater' unit, kappa = 0.99,  $P < 0.001$ .

In the multiple logistic regression analysis (included variables: SUVmax, SUVratio, and VUI), VUI ( $\chi^2$ : 33.411;  $P < 0.001$ ) was an independent predictor for PVE adjusted by age and PV type, yielding a diagnostic sensitivity, specificity and accuracy (95% CI) of 83% (71.9–90.7%), 93.3% (85.3–97.1%), and 88.9% (82.5–93.2%), respectively. A cut-off value of VUI > 0.45 improved PVE diagnostic yield, with 85% (73.9–91.9%) sensitivity, 88% (78.7–93.6%) specificity, and 86.7% (79.9–91.4%) diagnostic accuracy. SUVmax and SUVratio also showed good global diagnostic ability (complete results in Table 2, Supplementary data online, Material II and Figure 4A).

### Incremental diagnostic power of combined qualitative and quantitative features

Mean  $\pm$  SD VUI values according to the FDG uptake pattern and final diagnosis are shown in Figure 4B. Only in a few cases the VUI slightly mismatched with the final diagnosis and are explained in Supplementary data online, Material III. The combination of the currently used PET/CTA diagnostic criteria for PVE with the new proposed measurement (VUI > 0.45) significantly increased the diagnostic ability of this technique for confirming endocarditis. The addition of a VUI > 0.45 to a focal pattern increased the diagnostic accuracy (CI) from 79.3% (71.7–85.2%) to 90.4% (84.2–94.4%), and the addition of a VUI > 0.45 to a heterogeneous pattern increased the accuracy from 72.6% (64.5–79.4%) to 86.7% (79.9–91.4%). Finally, anatomic complications had a diagnostic accuracy for PVE of 79.3% (71.7–85.2%), which increased to 86.7% (79–91%) when adding a VUI > 0.45 (Figure 4A and Table 2).

### Metabolic findings according to the time from surgery to PET/CTA

Twenty-three (38%)/27 (36%) of the prostheses were implanted before 1 year and 37 (62%)/48 (64%) after 1 year in the 'definite' and the 'rejected' groups, respectively. There were no significant differences between any of the quantitative values before and 1 year after implantation in either the 'definite' or 'rejected' cases (mean  $\pm$  SD,  $</\geq 1$  year after implantation): SUVmax 8.21  $\pm$  3.11/7.36  $\pm$  3.04, SUVmean 3.31  $\pm$  0.9/3.04  $\pm$  1.01, SUVratio 4.23  $\pm$  1.7/4.42  $\pm$  2.46, and VUI 0.54  $\pm$  0.08/0.54  $\pm$  0.14 for the 'definite' group; SUVmax 3.94  $\pm$  0.95/3.61  $\pm$  1.18, SUVmean 2.52  $\pm$  0.62/2.3  $\pm$  0.72, SUVratio 2.41  $\pm$  1.2/2.01  $\pm$  0.72 and VUI 0.36  $\pm$  0.07/0.35  $\pm$  0.08 for the 'rejected' group. Of note, FDG uptake was visually detectable in only 33% (16/48) of 'rejected' cases when PV was implanted  $\geq 1$  year. Nevertheless, the uptake pattern in these cases was diffuse/homogeneous in 81% (13/16).

### Correlation between metabolic activity and the presence of anatomic lesions

Patients with 'definite' PVE and no anatomic lesions ( $n = 21$ ) had a lower mean SUVmax of 5.96  $\pm$  2.21 ( $P < 0.0001$ ), SUVratio 3.04  $\pm$  0.72 ( $P < 0.001$ ) and VUI 0.47  $\pm$  0.09 ( $P < 0.001$ ) than patients with at least one lesion ( $n = 39$ ): 8.61  $\pm$  3.09, 4.95  $\pm$  2.04, and 0.58  $\pm$  0.08, respectively (if divided in patients with only 1 lesion and

those with >1 lesions, values were 7.72  $\pm$  2.74/4.56  $\pm$  1.82/0.56  $\pm$  0.09 vs. 9.45  $\pm$  3.23/5.32  $\pm$  2.22/0.60  $\pm$  0.08).

There were no differences in SUVmax and VUI values among 'rejected' cases ( $n = 75$ ) with ( $n = 7$ ) or without ( $n = 68$ ) anatomic lesions (3.68  $\pm$  1.1 vs. 3.73  $\pm$  1.1;  $P = 0.758$ ; and 0.37  $\pm$  0.08 vs. 0.34  $\pm$  0.07;  $P = 0.307$ , respectively). Fistula/leak was the most frequent lesion observed in the 'rejected' group. Surprisingly, most of them were found in PV without visually detectable FDG uptake (absent pattern), indicating that this association may be poorly suggestive of infection.

## Discussion

The results of this study show that patients with 'definite' PVE had significantly higher 'valve uptake index' (VUI) values (0.54  $\pm$  0.1) than those with rejected PVE (0.36  $\pm$  0.08) ( $P < 0.001$ ). A VUI cut-off value of >0.45 yielded a diagnostic accuracy of 86.7% to confirm PVE (85% sensitivity and 88% specificity). Currently used PET/CTA qualitative (uptake pattern and anatomic lesions) and quantitative (SUVmax and SUVratio) parameters also confirmed their utility for the diagnosis of infection. A higher PVE diagnostic accuracy was achieved by addition of the VUI to the qualitative parameters.

The VUI correlated with the visual metabolic pattern of FDG uptake. Low VUI values were associated with no visually detectable metabolic activity or with a diffuse-homogeneous uptake (considered normal patterns). A high VUI was associated with focal/multifocal or diffuse-heterogeneous uptake (highly suggestive of infection) (Figures 4B and 5). Therefore, the VUI constitutes a numerical representation of the distribution of metabolic activity, and can help to assess whether FDG uptake is homogeneous or heterogeneous, which is a key feature when evaluating the probability that PV metabolic activity corresponds or not to infection. Visual interpretation of PET/CTA images is based on subjective evaluation, and some cases of diffuse uptake may be difficult to interpret. This becomes especially evident when uptake is very intense, which has been described as normal in some PV types,<sup>13</sup> and metabolic activity may not be completely expressed by the SUVmax or SUVratio, which express more the intensity of the uptake. The VUI attenuates the effect of high SUV values when uptake tends to be diffuse, reinforcing the visual interpretation of homogeneous, and probably not pathological, metabolic activity. In addition, an association was observed between the degree of FDG uptake and the presence of IE-related anatomic lesions. Higher VUI values correlated with a higher frequency of anatomic lesions in general, and with a higher frequency of periprosthetic complications.

The VUI can help to finally determine the pattern of FDG uptake in doubtful cases, compensating for the effect of extreme values of SUV—which can be subject to variability—on visual evaluation. In addition, the VUI is correlated with the presence of anatomical lesions and periprosthetic complications. Therefore, 'the VUI integrates both qualitative and quantitative information into a single numerical value' and would add consistency to the already established imaging criteria, increasing the diagnostic yield of PET/CTA. In addition, given the well-known problem of the lack of standardization of semi-quantitative measures, the VUI could be a parameter less influenced by technical differences, equipment or protocols, which can



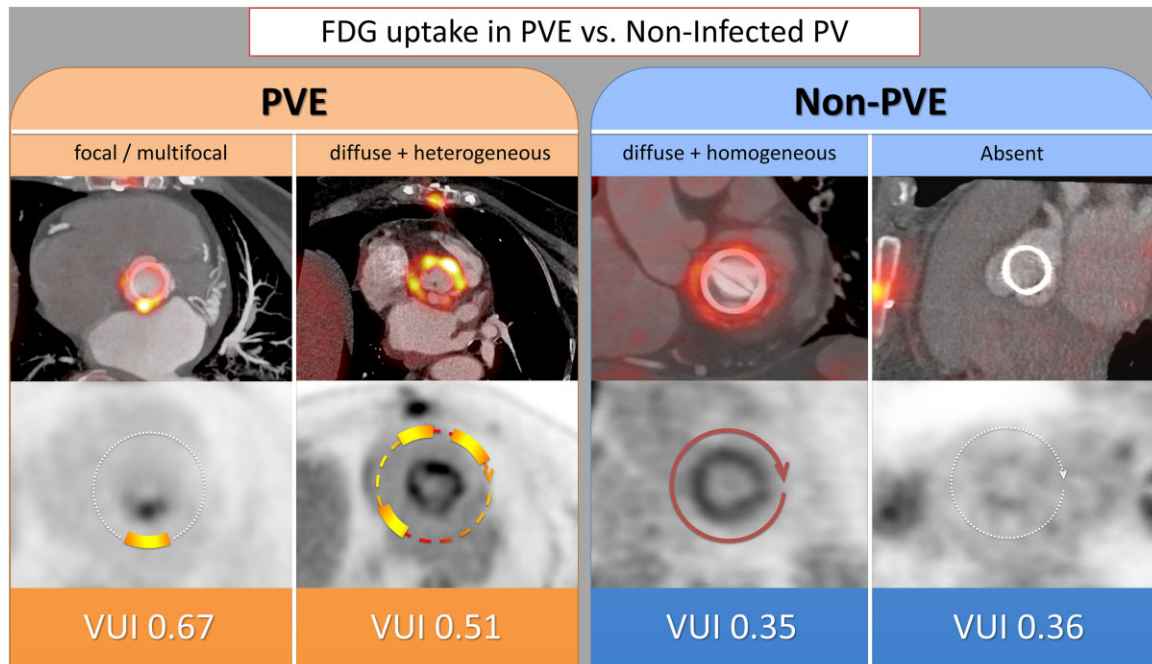


**Figure 5** FDG uptake distribution patterns (visual assessment) and their correlation with VUI values. FDG uptake in infected prostheses (PVE, left panel), compared with non-infected prostheses (non-PVE, right panel). PET/CTA fusion images of the valve plane (upper row), and their corresponding attenuation-corrected PET images (lower row), on which FDG distribution has been schematically represented. High VUI values correlate with focal/multifocal or diffuse+heterogeneous uptake patterns, which are highly suggestive of infection, whereas low VUI values reflect a diffuse+homogeneous pattern or absence of visually detectable FDG uptake, more characteristic of inflammation. FDG, fluorodeoxyglucose; PET/CTA, positron emission computed tomography angiography; PVE, prosthetic valve endocarditis; VUI, valve uptake index.

affect the absolute values of the SUV. This would make the VUI a potentially exportable measure between different centres and equipment. However, further studies are needed to validate this potential reproducibility. Finally, obtaining this parameter does not imply any change in either image acquisition or reconstruction, since it is calculated directly from the available SUV values.

No significant differences were seen in the VUI values according to valve type (mechanical or biological) or position (aortic or mitral) in either the definite or the rejected group, as previously reported in patients with no suspicion of IE.<sup>5</sup> Prosthetic/periprosthetic FDG uptake was visually detectable in all cases (100%) of 'definite' PVE, but in only 35% of the 'rejected' group, a frequency markedly lower than that reported in prostheses without suspicion of infection (79.3%). In addition, quantitative values of metabolic activity were lower in rejected cases than in those reported in postsurgical cases without suspicion of PVE (SUVmax  $3.72 \pm 1.11$  vs.  $4.46 \pm 1.50$ , SUVmean  $2.38 \pm 0.7$  vs.  $2.80 \pm 0.62$ , and SUVratio  $2.16 \pm 0.95$  vs.  $2.28 \pm 0.91$ ). These differences could be explained because PV controls in our previous study were scanned within the first year after implantation, while the median time from surgery to PET/CTA was 49 months in rejected PVE patients. The known metabolic activity due to postoperative inflammation may be higher in the recent post-implantation period and, although not well established, may gradually decrease over time. Irrespective of this consideration, a normal uptake pattern (absent or diffuse-homogeneous) was seen in 96% of patients in the

rejected group and in 93% of the control group. Likewise, the VUI, which in essence reflects FDG distribution, was superimposable, being  $0.35 \pm 0.08$  and  $0.35 \pm 0.10$ , respectively. A pathological uptake pattern (focal/multifocal or diffuse-heterogeneous) was seen in 97% cases in the definite PVE group.

## Diagnostic algorithm and criteria of PVE

The diagnostic approach by PET/CTA of a suspected PVE should include, when possible, both local assessment of the infection at the cardiac level (which will provide major diagnostic criteria), as well as extracardiac evaluation to determine the presence of distant lesions (minor criterion).<sup>4,14</sup> In addition, PET/CTA allows the identification of the source of infection, or an alternative diagnosis if PVE is ruled-out, both highly useful for patient management. Nevertheless, the main challenge remains the diagnosis of PV infection, often in a scenario in which echocardiographic evaluation is doubtful or negative, probably leading the definitive diagnosis of endocarditis to be established by PET/CTA.<sup>3,4</sup>

PET/CTA evaluation is based on metabolic and anatomical imaging criteria: the visual assessment of the location and distribution pattern of FDG uptake (visual analysis), the intensity of the uptake values (quantitative analysis), the presence or absence of anatomical lesions

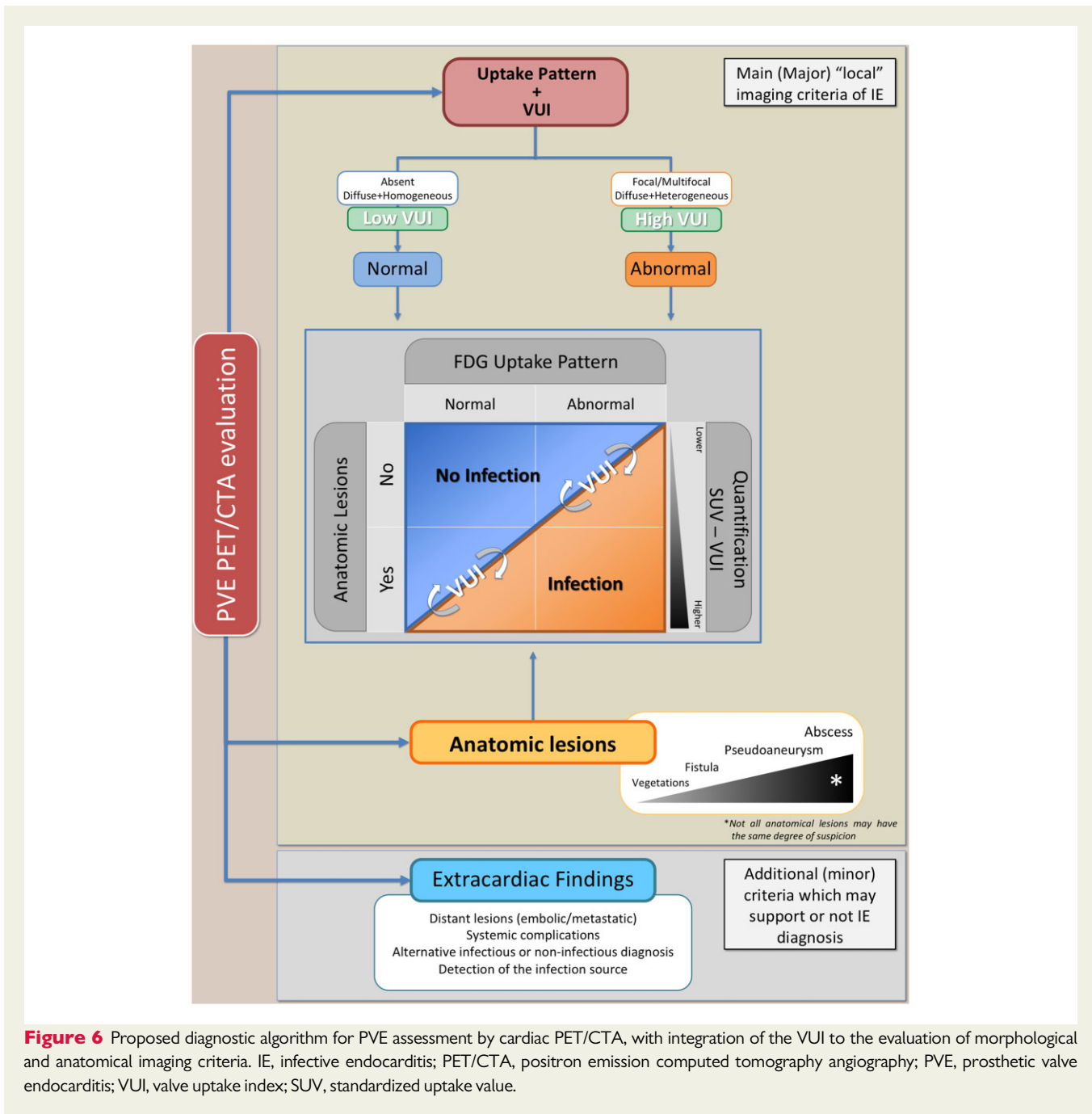


**Figure 6** Proposed diagnostic algorithm for PVE assessment by cardiac PET/CTA, with integration of the VUI to the evaluation of morphological and anatomical imaging criteria. IE, infective endocarditis; PET/CTA, positron emission computed tomography angiography; PVE, prosthetic valve endocarditis; VUI, valve uptake index; SUV, standardized uptake value.

related to IE in the CTA, and the correlation between the metabolic and anatomic images. Integrating the results of this study and the previously available knowledge, we have designed an improved diagnostic algorithm for PVE (Figure 6).

The key step in the diagnostic algorithm will be to define if the pattern of FDG uptake is 'normal' or 'abnormal'. Absent uptake or a diffuse and homogeneous uptake should be considered a 'normal' pattern. In contrast, a focal uptake or a diffuse and heterogeneous uptake will be highly indicative of infection ('abnormal' pattern). While focal FDG uptake should offer few diagnostic doubts, the challenge in classification would lie between the diffuse-homogeneous and diffuse-heterogeneous patterns. Due to its demonstrated good

correlation with the uptake distribution, the VUI could contribute to a correct interpretation of these difficult patterns, reinforcing visual interpretation. Moreover, the addition of the VUI to the uptake pattern has shown a significant increase in the diagnostic ability for PVE. In this regard, it may provide an important benefit in patients with multiple prostheses, or in situations where the uptake pattern may be subject to changes over time due to separate episodes of suspected IE or in follow-up scans (Figure 7 and Supplementary data online, Figure S1). In addition, the FDG uptake pattern, the traditionally used quantitative measures (SUVmax and SUV ratio) and the presence or absence of anatomic lesions have confirmed their usefulness in clinical practice.

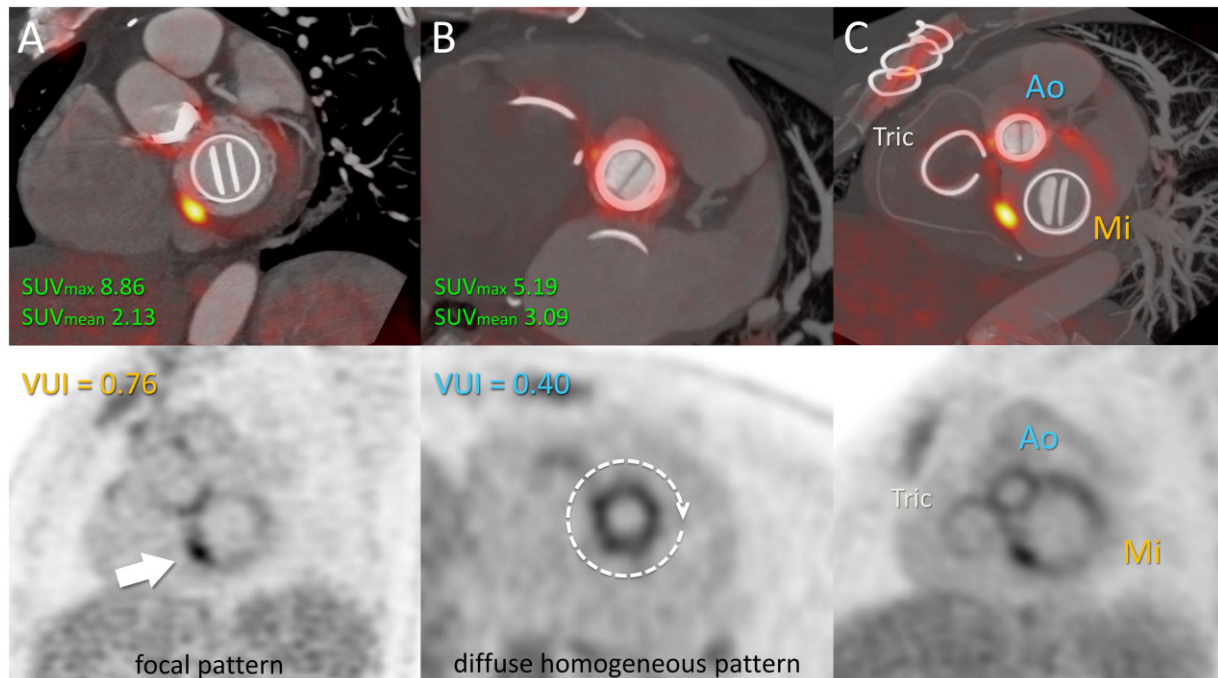


**Figure 7** Added value of the VUI in a patient with multiple PVs. A 45-year-old woman who had undergone aortic and mitral valve replacement and tricuspid annuloplasty 4 years previously was admitted due to fever and positive blood cultures for *Aggregatibacter aphrophilus* (HACEK group). Transoesophageal echocardiography was negative. (A) fused PET/CTA view of the mitral plane showed focal and intense FDG uptake ( $SUV_{max}$  8.86) in the inferoseptal aspect of the prosthetic ring-suture, with a VUI of 0.76, findings consistent with mitral PVE. (B) Aortic PV displays diffuse uptake of moderate intensity ( $SUV_{max}$  5.19), but with a low VUI of 0.40, indicating a homogeneous distribution, suggesting reactive inflammation and not supporting infective involvement. (C) Maximum intensity projection oblique plane including all cardiac PVs in a single view allows global assessment of the loco-regional distribution of metabolic activity. Focality is seen only over the mitral valve in contrast with the homogeneous distribution along the fibrous ring of the heart. Ao, aortic prosthetic valve; FDG, fluorodeoxyglucose; Mi, mitral prosthetic valve; PET/CTA, positron emission computed tomography angiography; PVE, prosthetic valve endocarditis;  $SUV_{max}$ , maximum standardized uptake value; Tri, tricuspid annuloplasty; VUI, valve uptake index.

Based on the results obtained, we propose a series of metabolic and anatomic ‘diagnostic criteria’ for PVE diagnosis by PET/CTA: (i) abnormal FDG uptake pattern: focal/multifocal or diffuse/heterogeneous uptake; (ii)  $SUV_{max} > 5.28$ ;  $SUV_{ratio} > 2.58$ ; (iii)  $VUI > 0.45$ ; and (iv) Presence of IE-related anatomic lesions, especially those that indicate periprosthetic extension of infection. The addition of extracardiac lesions to the main imaging criteria will support the diagnosis of IE.

Potential limitations of this study are: (i) although the VUI is a relatively simple value to calculate, this new parameter was obtained in a single centre with extensive experience on cardiac PET/CTA imaging and therefore its ultimate applicability must be verified through its use by other imaging readers. Likewise, as the VUI is obtained from a ratio between  $SUV_{max}$  and  $SUV_{mean}$ , it could correct certain differences derived from the lack of standardization in the acquisition and reconstruction of PET/CT images, as well as differences between equipment from different vendors. This possibility should be validated in further studies; (ii) although not a direct limitation of the present study, next step would be to evaluate the performance of the VUI in reclassifying patients with

an unclear visual pattern hence improving diagnosis. (iii) The proposed diagnostic algorithm includes searching for potential IE-related anatomic lesions, which can only be assessed if an associated ECG-gated cardiac CTA is performed, highly recommended whenever possible.

In conclusion, the VUI has demonstrated to be a valid and helpful parameter for PVE diagnosis. Because of its simplicity and potential reproducibility, it could be incorporated as a complementary tool into routine PET/CT evaluation, even when performed by less-experienced imaging readers. This study also confirms the utility of the most widely used parameters to date, both qualitative (uptake pattern and anatomic lesions) and quantitative ( $SUV_{max}$  and  $SUV_{ratio}$ ) for the diagnosis of infection. As the VUI provides both qualitative and quantitative information, its integration into the already established imaging criteria could improve the diagnostic yield of PET/CTA.

## Supplementary data

Supplementary data are available at *European Heart Journal - Cardiovascular Imaging* online.

## Acknowledgements

The authors thank the Hospital Universitari Vall d'Hebron Endocarditis Team: Benito Almirante, MD, PhD, Laura Escolà-Vergé, MD, PhD, Rubén Fernández, MD, Nuria Fernández-Hidalgo, MD, PhD, MSc, Maria Teresa González-Alujas, MD, Olga Maisterra, MD, PhD, Gerard Oristrell, MD, María Nazarena Pizzi, MD, PhD, Pau Rello, MD, Remedios Ríos, MD, PhD, Albert Roque, MD, Antonia Sambola, MD, PhD, and Toni Soriano, MD.

**Conflict of interest:** none declared.

## References

- Pizzi MN, Roque A, Fernández-Hidalgo N, Cuéllar-Calabria H, Ferreira-González I, González-Alujas MT et al. Improving the diagnosis of infective endocarditis in prosthetic valves and intracardiac devices with 18F-FDG-PET/CT-angiography: initial results at an infective endocarditis referral center. *Circulation* 2015;**132**:1113–26.
- Saby L, Laas O, Habib G, Cammilleri S, Mancini J, Tessonier L et al. Positron emission tomography/computed tomography for diagnosis of prosthetic valve endocarditis increased valvular 18F-fluorodeoxyglucose uptake as a novel major criterion. *J Am Coll Cardiol* 2013;**61**:2374–82.
- Habib G, Lancellotti P, Antunes MJ, Bongiorni MG, Casalta JP, Del Zotti F et al.; ESC Scientific Document Group. 2015 ESC Guidelines for the management of infective endocarditis: The Task Force for the Management of Infective Endocarditis of the European Society of Cardiology (ESC). Endorsed by: European Association for Cardio-Thoracic Surgery (EACTS), the European Association of Nuclear Medicine (EANM). *Eur Heart J* 2015;**36**:3075–128.
- Otto CM, Nishimura RA, Bonow RO, Carabello BA, Erwin JP III, Gentile F et al. 2020 ACC/AHA guideline for the management of patients with valvular heart disease: report of the American College of Cardiology/American Heart Association Joint Committee on Clinical Practice Guidelines. *Circulation* 2021;**143**:e72–227.
- Roque A, Pizzi MN, Fernández-Hidalgo N, Permanyer E, Cuellar-Calabria H, Romero-Farina G et al. Morphometabolic post-surgical patterns of non-infected prosthetic heart valves by [18F]FDG PET/CTA: "normality" is a possible diagnosis. *Eur Heart J Cardiovasc Imaging* 2020;**21**:24–33.
- Pizzi MN, Roque A, Cuéllar-Calabria H, Fernández-Hidalgo N, Ferreira-González I, González-Alujas MT et al. Infective versus inflammatory patterns in 18F-FDG-PET/CTA of prosthetic cardiac valves and valve-tube grafts. *JACC Cardiovasc Imaging* 2016;**9**:1224–7.
- Mathieu C, Mikail N, Benali K, lung B, Duval X, Nataf P et al. Characterization of 18F-fluorodeoxyglucose uptake pattern in noninfected prosthetic heart valves. *Circ Cardiovasc Imaging* 2017;**10**:e005585.
- Swart LE, Gomes A, Scholtens A, Sinha B, Tanis W, Lam M et al. Improving the diagnostic performance of 18F-FDG PET/CT in prosthetic heart valve endocarditis. *Circulation* 2018;**138**:1412–27.
- Scholtens AM, Swart LE, Kolste H, Budde R, Lam M, Verberne H. Standardized uptake values in FDG PET/CT for prosthetic heart valve endocarditis: a call for standardization. *J Nucl Cardiol* 2018;**25**:2084–91.
- Aguadé-Bruix S, Roque A, Cuéllar-Calabria H, Pizzi MN. Metodología de la 18F-FDG PET/CT cardíac para el diagnóstico de la endocarditis protésica y de dispositivos intracardiácos. *Rev Esp Med Nucl Imagen Mol* 2018;**37**:163–71.
- Roque A, Pizzi MN, Cuéllar-Calabria H, Aguadé-Bruix S. 18F-FDG-PET/CT angiography for the diagnosis of infective endocarditis. *Curr Cardiol Rep* 2017;**19**:15.
- Erba PA, Lancellotti P, Vilacosta I, Gaemperli O, Rouzet F, Hacker M et al. Recommendations on nuclear and multimodality imaging in IE and CIED infections. *Eur J Nucl Med Mol Imaging* 2018;**45**:1795–815.
- Roque A, Pizzi MN, Fernández-Hidalgo N, González-Alujas MT, Ríos R, Castell-Conesa J et al. Mosaic bioprostheses may mimic infective endocarditis by PET/CTA: trust the uptake pattern to avoid misdiagnosis. *JACC Cardiovasc Imaging* 2020;**13**:2239–44.
- Swart LE, Scholtens AM, Tanis W, Nieman K, Bogers A, Verzijlbergen F et al. 18F-fluorodeoxyglucose positron emission/computed tomography and computed tomography angiography in prosthetic heart valve endocarditis: from guidelines to clinical practice. *Eur Heart J* 2018;**39**:3739–49.